Charge Storage Behavior of Isotropic and Biaxially-Oriented Polypropylene Films Containing α- and β-Nucleating Agents

Nico Behrendt,[1] Nils Mohmeyer,[2] Joachim Hillenbrand,[3] Martin Klaiber,[3] Xiaoqing Zhang,[3] Gerhard M. Sessler,[3] Hans-Werner Schmidt,[2] Volker Altstädt[1]

[1]*Polymer Engineering, University of Bayreuth, D-95447 Bayreuth, Germany*
[2]*Macromolecular Chemistry I, University of Bayreuth, D-95447 Bayreuth, Germany*
[3]*Institute for Communications Technology, University of Technology Darmstadt, D-64283 Darmstadt, Germany*

Received 28 December 2004; accepted 31 March 2005
DOI 10.1002/app.22502
Published online in Wiley InterScience (www.interscience.wiley.com).

ABSTRACT: A study on the influence of the crystal modification (α and β) of isotactic polypropylene (i-PP) films on the resulting electret properties is presented. Two commercial nucleating agents, sodium 2,2′-methylene-bis(4,6-di-*tert*-butylphenyl)-phosphate (NA11) and N,N′-dicyclo-hexyl-2,6-naphthalene-dicarbox-amide (NU100), were employed in this investigation. Isothermal charge decay was measured at 90°C. In hot pressed isotropic polypropylene films, no significant differences in the charge storage properties were observed for α- and β-nucleated specimens. In addition, the article presents the influence of the nucleating agents at different concentrations on the PP-film morphology of biaxially stretched films with respect to electret features. It was possible to prepare elongated cavities with the virtually insoluble NA11 additive during stretching, even at concentrations below 0.3 wt %. These films displayed slightly improved electret properties in comparison to stretched neat PP films due to generated cavities acting as barriers for the drift of charges. Various draw ratios were also studied for i-PP films with 0.15 wt % NA11. © 2005 Wiley Periodicals, Inc. J Appl Polym Sci 99: 650–658, 2006

Key words: charge transport; drawing; films; nucleation; poly(propylene) PP

INTRODUCTION

Electrets are materials that exhibit a quasi-permanent electrical charge or polarization as a result of an external charging process.[1–3] The subsequent charge storage capability of polymeric materials is a consequence of traps, which prohibit or retard charge drift through the volume. Since the development of the electret-microphone,[4] electret materials have gained significant attention in a large number of technical applications, such as transducers, relay switches, sensors, electrostatic films, and filter units.[5] The most important polymer-electret materials are based on poly(tetrafluoroethylene) (PTFE) and its copolymers, which exhibit a good charge storage capacity as well as an outstanding charge stability. However, the beneficial properties of PTFE are restricted by the complicated and limited processing methods. Therefore, considerable attention is focused on thermoplastic polymers, such as cycloolefine copolymers (COC)[6] and isotactic polypropylene (i-PP).[7] The polymer morphology and impurities play an important role on the resulting electret features. The concentration and nature of traps in semicrystalline materials are expected to depend on factors such as amorphous-to-crystalline boundaries, defect sites, and impurities. For example, in the case of semicrystalline PP, Nath et al.[8] observed that the half-life period of the charge-decay temperature increased with an increasing degree of crystallinity upon annealing. Recently, the addition of special nucleating agents based on triphenylamide derivatives at optimal concentration was found to influence the charge storage properties of polypropylene films.[9] In addition, the mechanical deformation of films is a possibility to improve the charge storage behavior of semicrystalline polymers.[10,11] Here, it is assumed that the drawing influences the amorphous and crystalline morphology, and thereby increases the number and efficiency of traps. A different concept for the development of improved electret materials is the implementation of cavities. This approach is applied for PTFE,[12–14] and improvements in the charge decay behavior are explained by the obstruction of the charge drift by the cavities within the film. The formation of cavities in films is possible by drawing of plates, containing suitable particles.[15]

The aim of the present work is to investigate the influence of the crystal morphologies of i-PP on the charge storage properties. Two commercial nucleating

Correspondence to: N. Behrendt (nico.behrendt@uni-bayreuth.de).

agents, sodium 2,2′-methylene-bis(4,6-di-*tert*-butylphenyl)phosphate (NA11), inducing the α-modification,[16–20] and N,N′-dicyclohexyl-2,6-naphthalene-dicarboxamide (NU100), inducing predominantly the β-modification,[21–23] were selected. Hot pressed films and biaxially stretched films were investigated in this study.

EXPERIMENTAL

Materials

An isotactic polypropylene reactor powder, supplied by Borealis Linz, Austria, was used for the investigations. The weight average molecular weight was 425,000 g/mol, with a polydispersity of 3.5. As nucleating agents, 2,2′-methylene-bis(4,6-di-*tert*-butylphenyl)-phosphate (NA11) from Asahi Denka Kogyo K.K. Tokyo, Japan and N,N′-dicyclohexyl-2,6-naphthalene-dicarboxamide (NU100) from New Japan Chemical Company were used. The particle size distribution of as-received NA11 particles dispersed in isopropanol was determined by laser light scattering (Helium-Neon-Laser, λ = 632.8 nm), using a CILAS 715, as d_{10} = 5.05 μm, d_{50} = 15.64 μm, and d_{90} = 41.9 μm.

Specimen preparation

Isotropic films. Polymer/additive mixtures were prepared in a laboratory, corotating mini-twin-screw extruder (Technical University Eindhoven, The Netherlands) at 240°C under nitrogen for 4 min. The extruded mixtures were subsequently melted at 260°C under nitrogen for 2 min and injection molded using a micro-injector (DACA Instruments, Goleta, CA), yielding a specimen of 1.1 mm thickness and 25 mm diameter. 50 μm thick films were prepared by hot pressing these compression molded specimens between Kapton®-foils and metal plates by melting at 260°C for 3 min and pressing during 4 min at 15 kN in a laboratory press (P.O. Weber 10 H), followed by cooling down to room temperature between 2 mm thick metal plates at room temperature.

Stretched films. The i-PP-powder and the additives, both NA11 and NU100 at concentrations of 0.05, 0.15, and 0.3 wt %, were mixed at room temperature in a MTI LM 2.5 FU laboratory universal mixer at 900 rpm under nitrogen for 9 min. The dry powder mixtures were then fed into a single-screw Collin lab-extruder (screw diameter 20 mm, aspect ratio of 25), operating at 200°C (1st to 3rd heating zone) and 230°C (die temperature). The screw speed was 25 rpm. Rectangular sheets of 100 mm width and a thickness of 0.3 mm were obtained using a slit die. The thin sheets extruded into air were wound up using a chill roll system (roll temperature: 8°C, haul-off speed 12 m/min). Square samples of 50 mm × 50 mm were cut from the central part of the extruded sheets. Stacks of 12 sheets were subsequently hot-pressed to 0.9 mm thick plates between 100 μm Kapton®-foils and two 2 mm thick metal plates using a P.O. Weber lab press. After 3 min of preheating at 260°C without pressure, a constant force of 15 kN was applied for 4 min at this temperature, followed by cooling down to room temperature outside the hot-press between the metal plates. The dimensions of the hot-pressed plates were 100 mm × 100 mm, from which 85 mm × 85 mm samples were cut. Stretched films were prepared from the hot-pressed plates by clamping them between thimbles and simultaneous biaxial stretching in a Brückner laboratory-scale film-stretcher (KARO IV), operating at 155°C. A detailed description of the stretching procedure using this set-up can be found in Capt et al.[24] At first, the plates were heated up in the framework at 155°C for 40 s. A constant strain rate of 50 mm/s was used. The final dimensions of the stretched films were 270 mm × 270 mm × 0.05 mm. The applied stretch ratio of samples containing different weight fractions of both NA11 and NU100 was 1: 3.5 in the machine (MD) and transverse direction (TD). In addition, different draw ratios were applied for i-PP samples containing 0.15 wt % of NA11. The respective draw-ratios of the samples containing 0.15 wt % of NA11 are listed in Table I. The thickness of the final films was adjusted to be about 50 μm. This was achieved by using compression molded plates with a different thickness.

TABLE I
Overview of the Applied Draw Ratios of i-PP Films Comprising 0.15 wt % NA11

Symmetric (MD = TD) Asymmetric (MD = TD)	Machine direction (MD)	Transverse direction (TD)
symmetric	1 : 2.5	1 : 2.5
symmetric	1 : 3.5	1 : 3.5
symmetric	1 : 7	1 : 7
asymmetric	1 : 1.5	1 : 5.5
asymmetric	1 : 2.5	1 : 4.5
asymmetric	1 : 1	1 : 6

Specimen characterization

The crystallization behavior of the isotropic i-PP films containing different concentrations of the nucleating agents NA11 and NU100 was investigated by polarized light microscopy, using a Nikon Diaphot 300. Samples for optical microscopy were prepared by placing a piece of the extruded polymer/additive mixture onto a glass slide, then melting and protecting with a cover glass. Micrographs were taken between crossed polarizers using a Nikon microscope equipped with a hot-stage (Mettler Toledo FP82HT). Standard scan rates were 5°C/min.

TABLE II
Thermal Properties of Unstretched (us) and Stretched (s) i-PP Films Nucleated with Different Concentrations of NA 11

NA11 (wt %)	Melting peak temperature (°C) 1st heating		Degree of crystallinity (%) 1st heating		Crystallization peak temperature (°C) 1st cooling
	us	s	us	s	us
0	158.7	164.0	49	49	112.2
0.05	162.7	164.5	50	48	125.3
0.15	164.5	165.2	47	50	130.2
0.30	164.1	167.2	50	50	131.6

The measurements to probe the nucleation efficiency of the compounds were performed with samples of 8–10 mg at a heating and cooling rate of 10°C/min under nitrogen starting from 0 to 230°C, annealing at 230°C for 5 min to ensure the complete melting of the polymer, followed by cooling down to 0°C. The maximum of the crystallization exotherm is listed as the crystallization temperature (T_c) in Tables II and III. The degree of crystallinity, X_c, was calculated from the melting enthalpies normalized to the actual weight fraction of the polymer according to eq. (1):

$$X_c = \left(\frac{\Delta H_m}{\Delta H_m^0} * W_{Polymer}\right) * 100$$

with $\Delta H_m^0 = 207$ J/g, the theoretical value of melting enthalpy for 100% crystalline polypropylene,[25] and $W_{Polymer}$ is the weight fraction of the polymer matrix. The degree of crystallinity was determined with experimental accuracy of 1%.

Wide angle X-ray diffraction (WAXD) measurements were carried out on both the isotropic and oriented films to determine the polymorph composition. Stacks of eight films were clamped into a holder and characterized in transmission using CuKα-radiation, $\lambda = 0.15{,}418$ nm (Bruker-AXS D8 Advance). All films were mounted in the same way with respect to the radiation source. The geometry of the radiation source slot was 2.0×1.0 cm^2. The step-size of the detector was set at 0.025° between 8 and 30° for 2θ.

The microstructure of the oriented i-PP films after the drawing process was investigated using a JEOL JSM-IC 848 scanning electron microscope (SEM), operating at 15 kV. Fracture surfaces were prepared under liquid nitrogen and subsequently sputtered with gold using a Cressington Sputter Coater 108.

Charge storage properties

Films of 8cm × 5cm area and about 50 μm thickness of the different polypropylene/additive mixtures were glued onto aluminum plates with conductive double-side adhesive tape. Conductive tape was used as an electrode because preparatory experiments had shown that such samples exhibit better charge stability than films metallized on one side by Al evaporation, as generally employed for isothermal charge decay experiments.[1] The better stability is probably due to the fact that charge injection is absent with this kind of electrode.

All samples were charged for 60 s using a point-to-plate corona setup with a grid for limitation of the surface potential. Corona voltages of +12.5 kV and grid voltages of +400 V were employed. The surface potential of each sample was measured at six well-defined positions with an electrostatic voltmeter (Trek Model 369). In some cases measurements were repeated on a second identical sample. Since the results were reproducible, it was not necessary to repeat measurements for all samples. Measurements were performed directly after charging at room temperature

TABLE III
Thermal Properties of Unstretched (us) and Stretched (s) i-PP Films Nucleated with Different Concentrations of NU100

NU100 (wt %)	Melting peak temperature (°C) 1st heating		Degree of crystallinity (%) 1st heating		Crystallization peak temperature (°C) 1st cooling
	us	s	us	s	us
0	158.7	164.0	—	49	112.2
0.05	150.6/167.6	167.8	—	46	124.9
0.15	151.0/163.0	169.6	—	46	123.4
0.30	149.9/166.7	166.9	—	47	124.1

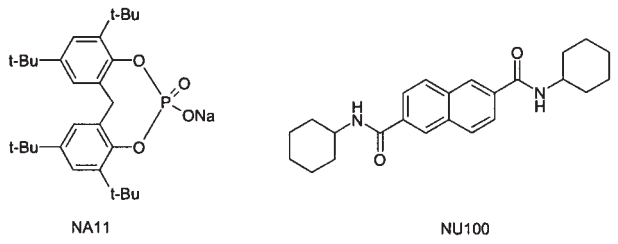

Figure 1 Chemical structures of sodium 2,2′-methylene-bis(4,6-di-*tert*-butyl-phenyl) phosphate (NA11) and N,N′-dicyclohexyl-2,6-naphthalene-dicarboxamide (NU100).

and after annealing at 90°C for cumulative periods of 10, 30, 60, 90, 180, and 360 min for the isotropic films and additionally at 720 and 1440 min for the orientated films. The potential measurements were performed at room temperature, outside the heating chamber since the electrostatic voltmeter could not be exposed to the high temperature and positioning of the sample for measurement would have been extremely difficult under these conditions. Thus, the samples were subjected to several heating and cooling cycles during the isothermal charge decay measurements. However, the cooling of the samples to room temperature has a negligible effect on their surface potentials, since charge transport processes are slowed down by orders of magnitude at room temperature compared to 90°C.

RESULTS AND DISCUSSION

Polymorph composition of nucleated i-PP films

The two commercial available nucleating agents NA 11 and NU100 (Fig. 1) were used to create the α- and β-modification of isotactic polypropylene. In the literature, the additives NA11[16–20] and NU100[21–23] were described as efficient nucleating agents in i-PP at low concentrations.

Melting and crystallization temperatures of the neat and nucleated polypropylene films were determined by differential scanning calorimetry (DSC) to show, on the one hand, the differences between the α- and β-modification and, on the other hand, the differences between the hot pressed and biaxially stretched polypropylene films. The degrees of crystallinity were calculated from the recorded nonisothermal DSC thermograms. The calculated values of X_c are normalized with respect to the weight fraction of the polymer matrix.

NA11 and NU100 modified films are clearly different in relation to their thermal properties. These varieties are pictured in Figure 2 in the form of DSC thermograms.

Unstretched neat i-PP displayed a melting peak temperature of 158.7°C. In the case of stretched neat i-PP, the melting peak temperature was found at 164.0°C. In comparison to the isotropic neat films, the unstretched i-PP containing 0.3 wt % of NA11 displays a melting peak temperature of 164.1°C and 167.2°C for the orientated film. In contrast to the NA11-nucleated i-PP films, the isotropic film containing 0.3 wt % NU100 showed a double melting peak during the first heating run. The presence of the first melting endotherm peak at about 149.9°C indicates the β-crystal structure, whereas the second melting peak at 166.7°C corresponds to the α-structure.[26,27] This double melting peak is exhibited by all unstretched i-PP films containing different concentrations of NU 100. However, the melting endotherm peak corresponding to the β-modification was not present for the oriented films, and only the regular α-melting feature at 166.9°C remained. This β-to-α transition of isotactic polypropylene upon drawing is in agreement with earlier investigations, as described in the literature.[28]

The thermal properties are summarized in Tables II and III. Melting peak and crystallization peak temperatures of stretched and unstretched films as a function of the additive weight fraction of NA11 are summarized in Table II. The degree of crystallinity was determined with experimental accuracy of 1%. No significant variation in the overall peak shape and degree of crystallinity with increasing weight fraction of NA11 could be found. The nonlinear increase in melting peak and crystallization peak temperature with increasing NA11 content for the concentration range studied here is known for the investigated system.[20] The degree of crystallinity appeared to remain constant within experimental accuracy at around 49%. An evaluation of the exact degree of crystallization from the first heating runs of the as-pressed films, has been omitted due to the polymorphism.

Results of thermal investigations for NU100 nucleated films are listed in Table III. However, in the case

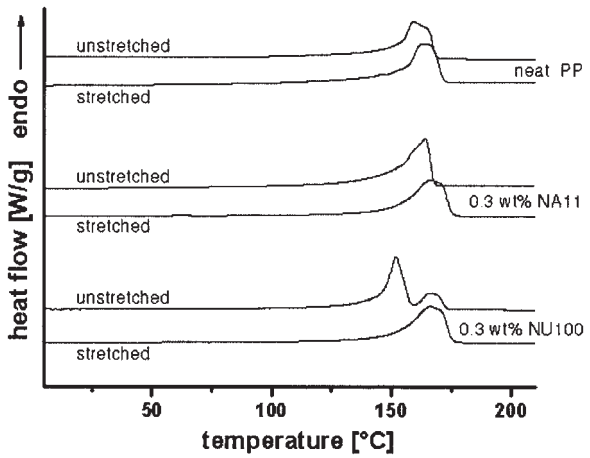

Figure 2 DSC thermograms of unstretched and stretched i-PP films and films containing 0.3 wt % of NA11 and 0.3 wt % NU100, respectively. Drawing conditions: ratio 3.5 (MD) : 3.5 (TD); deformation rate: 50 mm/s; temperature: 155°C.

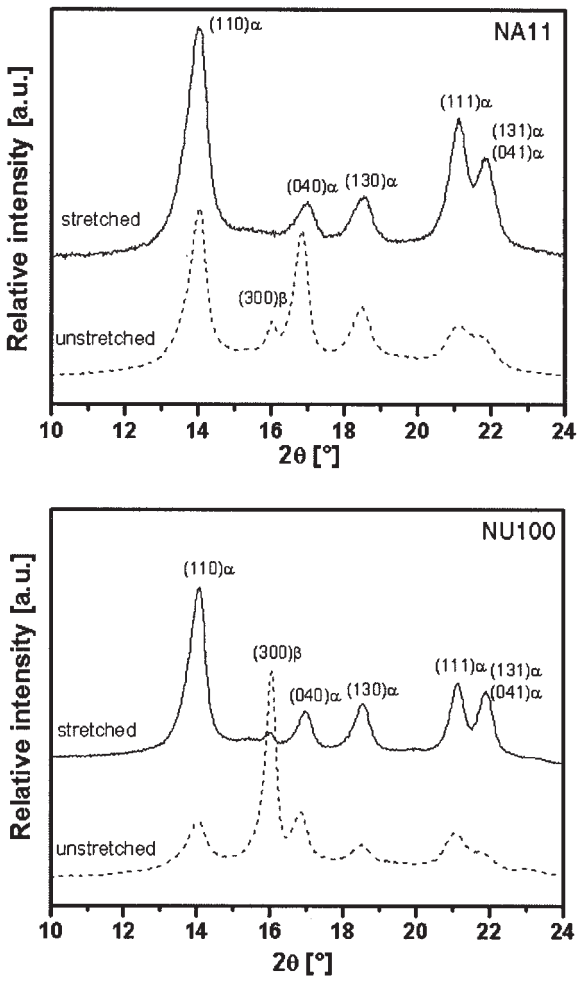

Figure 3 Wide angle X-ray diffraction (WAXD) patterns recorded at room temperature of unstretched and biaxially stretched i-PP films. Top: films containing 0.3 wt % of NA11; bottom: films containing 0.3 wt % of NU100. Drawing conditions: ratio 3.5 (MD) : 3.5 (TD); deformation rate: 50 mm/s; temperature: 155°C.

of NU100 nucleated films, no concentration dependence was observed. The typical double melting peak was found for all unstretched NU100 nucleated films. The degree of crystallinity of the stretched films varies between 46 and 49%.

Examples of complementary equatorial WAXD patterns are shown in Figure 3 for unstretched and stretched i-PP films containing 0.3 wt % of NA11 (top) and NU100 (bottom). All films were mounted in the same way with respect to the radiation source. Figure 3 (top) displays the intensity profiles as a function of 2θ for the i-PP films containing NA11, with characteristic reflections of α-PP[19] for both the unstretched (dotted line) as well as the stretched films (solid line). The intensity profile of the isotropic specimen containing 0.3 wt % NA11 shows a weak signal [lattice plane (300)] of the β-modification. Such small amounts of β-modification can be caused by the melt processing. Figure 3 (bottom) shows the coexistence of α- and β-crystal modifications in the isotropic i-PP films containing NU100, in agreement with the double melting feature observed in the DSC experiments. The lattice plane (300) in the diffractogram of the isotropic film containing NU 100 is indicative of the β-modification and can be used to differentiate between the two crystal structures.[27] The characteristic β-reflection evidently disappears upon drawing, which is in agreement with the DSC observations and the literature.[28,29]

Electret properties of the hot pressed isotropic i-PP films

Isothermal charge decay measurements at 90°C were carried out directly after charging. Again, the samples were removed from the oven after a fixed time period and were measured at room temperature. The resulting potentials for the six measurement positions (see above) were averaged and plotted as a function of annealing time. The charge storage efficiency of electrets is related to the mechanism of self-discharge, more precisely, the drift of electric charges through the volume as a function of time. In the case of PTFE, it has been demonstrated that the morphology plays an important role to influence the charge drift through the bulk.[12]

Figure 4 illustrates the time-dependent charge decay of the surface potential of the isotropic i-PP films containing 0.05, 0.15, and 0.3 wt % of NA11 (top) or NU100 (bottom) in comparison to the neat polypropylene. For both nucleating agents, NA11 and NU100, the charge decay was found to proceed faster in comparison to the neat i-PP reference. This effect was most pronounced for the film containing 0.05 wt % of NA11 (Fig. 4 top); the two higher additive concentrations of NA11 decreased the surface potential to a value of 200 V after 360 min annealing time. All NA11-nucleated films displayed after short times of annealing a lower surface potential in comparison to neat i-PP. However, the surface potentials decrease more slowly with higher concentrations at 0.15 and 0.3 wt % of NA11. It is assumed that the NA11 particles act as a barrier for the drift of charges. Probably, the barrier effect begins only after a certain time period of annealing, if some charges are directly moved before the particles. Then, electrostatic repulsion prevents a drift of the other charges from the surface into the volume.

Also, all NU100 containing films showed a substantial drop in surface potential compared to the polypropylene reference after annealing, although no systematic change with concentration could be observed. In the case of the NU100 nucleated films, the concentration-independent charge decay implies a different mechanism of self-discharge. Here, the chemical structure of the additive with the intermolecular formation of hydrogen bonds provides pathways for the charges

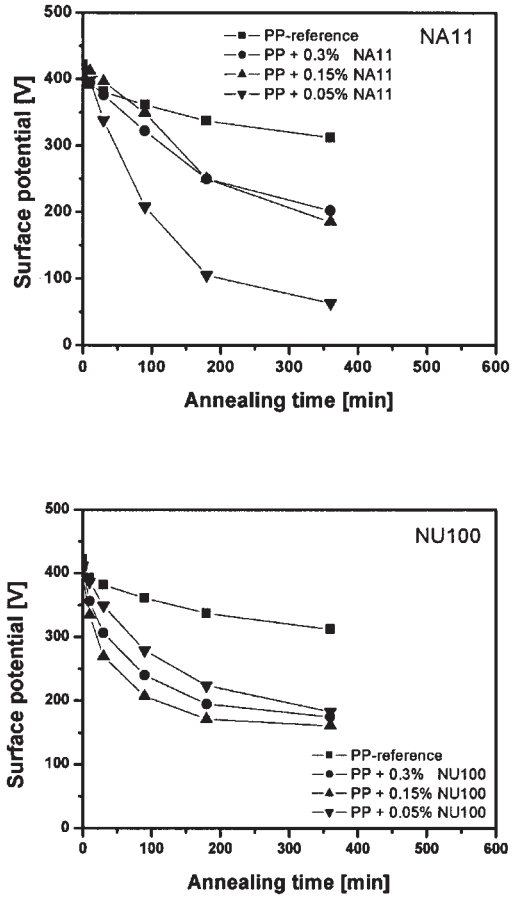

Figure 4 Surface potential as a function of the annealing time at 90°C of hot-pressed i-PP films (thickness: 50 μm) with different concentrations of NA11 (top) and NU100 (bottom) in comparison with the isotropic polypropylene reference.

through the volume of the film due to the formation of fibrillar three-dimensional network structures of the additive; compare Figure 5(c).[9]

Optical microscopy of nucleated i-PP films

The cross-polarized optical microscopy experiments in the molten state verified the uniform distribution of NA11 particles in the i-PP as a result of the processing. Figure 5(a) shows an optical micrograph of a specimen containing the highest investigated weight fraction of 0.3 wt % of NA11 in polypropylene, taken after cooling with a cooling rate of 5°C/min to 160°C. The virtually insoluble NA11 particles are visible as small white dots, which were also observed at the employed processing temperature of 260°C. Successive optical micrographs taken as a function of decreasing temperature showed an increasing onset temperature of crystallization with increasing weight fraction of additive, verifying the heterogeneous surface area nucleation of this additive.[19,20] Figure 5(b) shows the "fine-grained" morphology of i-PP containing 0.3 wt % of NA11 at 125°C, indicative of the strong nucleation ability of this particular additive.[16–20] It has even been shown that finely dispersed NA11 particles induce epitaxial growth of polypropylene α-crystals.[19] In contrast to the virtually insoluble NA11, NU100 exhibits partial solubility in molten i-PP. Upon cooling at a cooling rate of 5°C/min to a temperature of 160°C, formation of fine birefringent fibrillar structures was observed [Fig. 5(c)]. Upon further cooling to a temperature of 125°C, crystallization of i-PP onto the surface of the three-dimensional network structure of NU 100 was

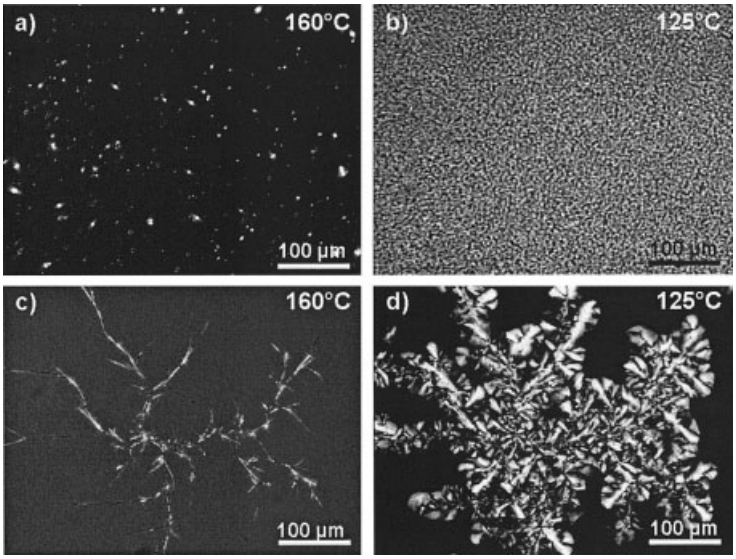

Figure 5 Optical micrographs, between crossed polarizers, of i-PP containing 0.3 wt % of NA11 (a, b) and 0.3 wt % of NU100 (c, d). (a) shows undissolved particles of NA11 in molten i-PP at 160°C; (b) the crystallized i-PP at 125°C induced by the nucleating agent NA11; (c) fibrillar structures of NU100 grown within the i-PP melt at 160°C; and (d) the crystallization of i-PP on the surface of the additive at 125°C.

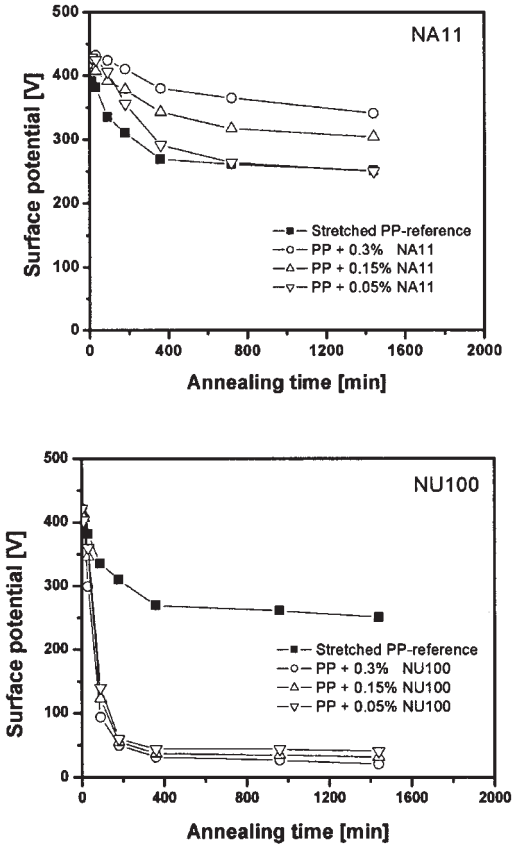

Figure 6 Surface potential as a function of annealing time at 90°C of biaxially stretched i-PP films (50 μm thick) with different concentrations of NA11 (top) and NU100 (bottom) in comparison with the biaxially stretched polypropylene reference. Drawing conditions: ratio 3.5 (MD) : 3.5 (TD); deformation rate: 50 mm/s; temperature: 155°C.

observed [Fig. 5(d)]. The appearance of the grown white spherulites indicates the β-modification of isotactic polypropylene. Similar observations were made during the investigation of triphenylamine-based trisamide derivates in i-PP.[9]

Electret properties of biaxially stretched porous i-PP films

It was determined that neat PP films display an improved electret behavior in a small range after drawing (Figs. 4 and 6). Furthermore, in Figure 6, the effect of biaxial drawing various i-PP films containing NA11 (top) and NU100 (bottom) on the resulting electret features is shown.

The surface potential of orientated films containing 0.05 wt % NA11 is similar to the potential of orientated neat PP after 720 min of annealing. However, as can clearly be seen, there is a slower decay in the measured surface potential of the oriented PP films containing 0.15 and 0.3 wt % NA11 in comparison to orientated neat PP (Fig. 6 top). On the contrary, the orientated films containing NU100 (Fig. 6 bottom) exhibited a dramatic decrease of the charge storage behavior, irrespective of the concentration. After annealing for 200 min, the measured surface potential dropped to 30 V. The strong decay of the surface potential may have been caused by connecting charge drift pathways, which could promote discharging in comparison to the isotropic nucleated films.

Scanning electron microscopy images of fracture surfaces were examined to gain a more profound understanding of the charge storage mechanism in relation to the employed additives and the stretching process (Fig. 7). The image of neat orientated i-PP is shown in Figure 7(a). In this case, a compact material is visible. A stretched film, containing 0.3 wt % NU

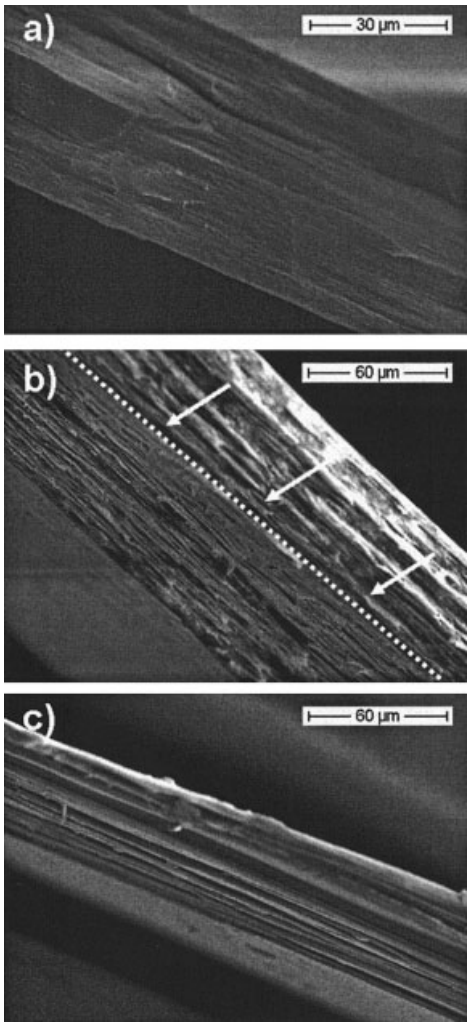

Figure 7 Scanning electron micrographs of fracture surfaces of biaxially oriented i-PP films. The micrographs show: (a) biaxially oriented neat i-PP-reference; (b) i-PP containing 0.3 wt % of NU100 (the white arrows and dotted line indicate the edge of the specimen); and (c) i-PP containing 0.3 wt % of NA11. The drawing parameters are the same in all cases: ratio 3.5 (MD) : 3.5 (TD); deformation rate: 50 mm/s; temperature: 155°C.

100, achieved small and short cavities, which are irregularly distributed in the material [Fig. 7(b)]. However, the fracture surface of NA11 nucleated films displays highly elongated and regular cavities [Fig. 7(c)]. The formation of these elongated cavities in the PP films containing the NA11 particles appears to result from weak interfacial bonding between the additive particles and the partially molten polymer. Upon stretching, the dispersed particles act as stress concentrators even in the material and lead to the formation of local microvoids. These local voids are subsequently enlarged during the drawing process, essentially leading to cavities hundreds of micrometers long within the plane of the film. The higher the additive concentration, the more local voids and subsequent large cavities are formed.[15]

A schematic representation of the mechanism by which these cavities enhance the electret features is shown in Figure 8. The improvement in charge storage behavior is achieved by the elongated cavities providing effective barriers for the charge drift through the film thickness.

These experimental observations as well as the proposed mechanism agree with results obtained for porous PTFE,[12–14] where local cavities were achieved by biaxial drawing of the base polymer.

Electret properties of porous i-PP films with 0.15 wt % NA11 stretched by different draw ratios

To supplement the previous investigations, a set of films based on i-PP, containing 0.15 wt % NA11, was subjected to different draw ratios (see Table I). The thickness of the final films was adjusted to be about 50 μm. This was achieved by using compression molded plates with a different thickness. The surface potential measurement results for symmetric (top) and asymmetric (bottom) draw ratios are shown in Figure 9. In general, with symmetric draw ratios, an improvement of the surface potential was found, which increases with increasing draw ratios. This enhancement is attributed to an enlargement of the cavities with increasing draw ratio. The high draw ratio of 7 : 7 leads to enlarged cavities in comparison to lower draw ratios. Thus, an improved barrier effect for charge drift is caused by enlargement of cavities.

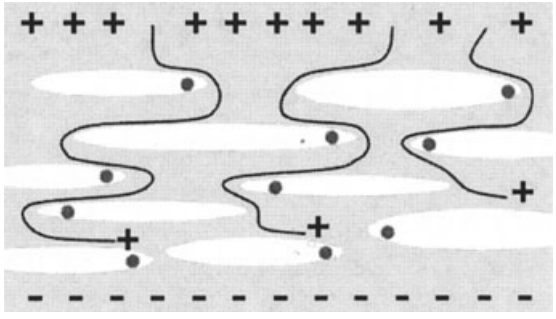

Figure 8 Schematic representation of charge drift obstruction in porous electrets by drawing-induced elongated cavities.

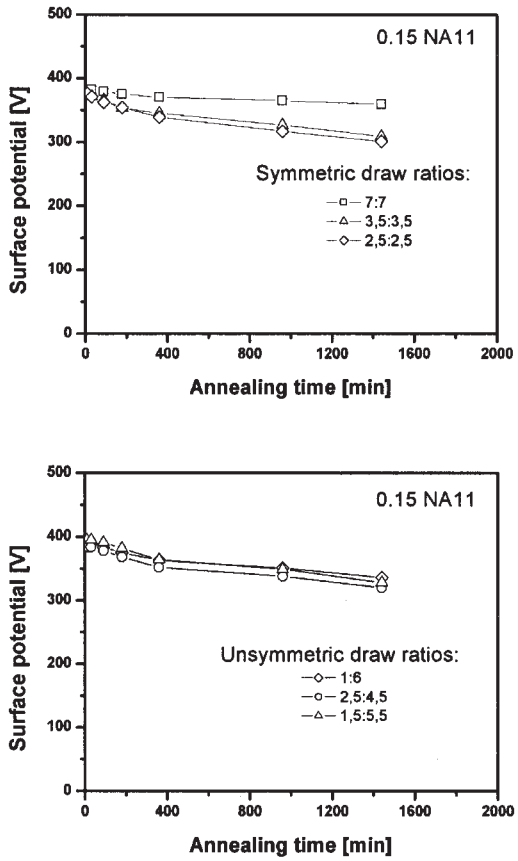

Figure 9 Influence of draw ratio on the surface potential as a function of annealing time at 90°C in the case of biaxially stretched i-PP films (thickness: 50 μm) with a concentration of 0.15 wt % NA11. The figures compare symmetrical (top) and unsymmetrical (bottom) stretched films. The drawing temperature was 155°C, and the deformation rate amounted to 50 mm/s.

However, with asymmetrical draw ratios, no significant differences were observed in the range of applied draw ratio.

CONCLUSIONS

In the present work, we have shown that adding two nucleating agents (NA11 and NU100) in isotropic i-PP films at concentrations 0.05 to 0.3 wt % decreases the charge storage properties in comparison to neat i-PP films. No difference of α- and/or β-modification on the charge storage properties could be determined.

However, in biaxial stretching of i-PP with the nucleating agent NA11, elongated cavities are formed during drawing within the plane of the films even at low concentrations. The development of these cavities under the chosen drawing conditions is caused

through the function of NA11 as a stress concentrator at low concentrations. These cavities provide effective barriers for the charge drift, resulting in slightly improved electret properties of i-PP films. Furthermore, the electret properties are also influenced by the draw ratio. An improvement of charge storage properties was determined with higher draw ratios.

The authors thank the Deutsche Forschungsgemeinschaft (DFG) for financial support of the project (DFG-Projekt Al 474/5–1; Schm 703/2–1, Se 325/22–1). Furthermore, we are indebted to the Institute of Polymeric Materials (Lehrstuhl für Polymere Werkstoffe), Prof. Dr. H. Münstedt, University of Erlangen, Germany, for access to the stretching frame. Mr. Marko Heyder especially is acknowledged for his support with the experimental work using this rig.

References

1. Sessler, G. M. Electrets; Springer: New York, 1999; Vol. I, 3rd ed.
2. Moreno, R. A.; Gross B. J Appl Phys 1976, 47, 3397.
3. Gross, B.; Sessler, G. M.; West, J. E. J Appl Phys 1977, 48, 4303.
4. Sessler, G. M.; West J. E. J Acoust Soc Am 1962, 34, 1787.
5. Sessler, G. M.; Gerhard-Multhaupt, R. Electrets; Laplacian Press: Morgan Hill, CA, 1999.
6. Yang, G. M.; Sessler, G. M.; Hatke, W. Proc Internat Symp Electr; Institute of Electrical and Electronics Engineers, Delphi, Greece 1999, 9, 317.
7. Yovcheva, T. A.; Mekishev, A. G.; Marinov, A. T. J Phys: Condens Matter 2004, 16, 455.
8. Nath, R.; Perlman M. M. IEEE Trans Electr Insul 1989, 24, 409.
9. Mohmeyer, N.; Müller, B.; Behrendt, N.; Hillenbrand, J.; Klaiber, M.; Zhang, X.; Smith, P.; Altstädt, V.; Sessler, G. M.; Schmidt, H.-W. Polymer 2004, 45, 6655.
10. Mittal, A.; Jain, V.; Mittal, J. J Mater Sci Lett 2001, 20, 681.
11. Jain, V.; Mittal, A. J Mater Sci Lett 1991 2000, 19.
12. Cao, Y.; Xia, Z.; Li, Q.; Shen, J.; Chen, L.; Zhou, B. IEEE Trans Dielectr Electr Insul 1998, 5, 58.
13. Xia, Z.; Wedel, A.; Danz, R. IEEE Trans Dielectr Electr Insul 2003, 10, 102.
14. Xia, Z.; Ma, S.; Qui, X.; Zhang, Y. J Electrostat 2003, 58, 265.
15. Nago, S.; Mizutani, Y. J Appl Polym Sci 1998, 68, 1543.
16. Mai, K.; Wang, K.; Han, Z. J Appl Polym Sci 2002, 83, 1643.
17. Gui, Q.; Xin Z.; Zhu, W. J Appl Polym Sci 2003, 88, 297.
18. Mai, K.; Wang, K.; Zeng, H. J Appl Polym Sci 2003, 88, 1608.
19. Yoshimoto, S.; Ueda T.; Yamanka, K. Polymer 2001, 42, 9627.
20. Marco, C.; Gomez, M. A.; Ellis G. J Appl Polym Sci 2002, 84, 1669.
21. Kotek, J.; Raab, M.; Baldrian, J. J Appl Polym Sci 2002, 85, 1174.
22. Kawai, T.; Iijima, R.; Yamamoto, Y. J Phys Chem B 2001, 105, 8077.
23. Kawai, T.; Iljima, R.; Yamamoto, Y. Polymer 2002, 43, 7301.
24. Capt, L.; Rettenberger, S.; Münstedt, H.; Kamal, M. R. Polym Eng Sci 2003, 43, 1428.
25. Cheng, S. Z. D.; Janimak, J. J.; Zhang, A. Polymer 1991, 32, 648.
26. Yuan, Q.; Jiang, W.; An, L. Colloid Polym Sci 2004, 282, 1236.
27. Vleeshouwers, S. Polymer 1997, 38, 3213.
28. Yang, W.; Li, Z.-M.; Xie, B.-H.; Feng, J.-M.; Shi, W.; Yang, M.-B. J Appl Polym Sci 2003, 89, 686.
29. Turner-Jones, A.; Aizlewood, J. M.; Beckeet, D. R. Macromol Chem 1964, 75, 134.